JOURNAL OF MATERIALS SCIENCE 17 (1982) 3299–3307

Superconducting properties of amorphous Zr–Ge binary alloys

A. INOUE, Y. TAKAHASHI*, N. TOYOTA, T. FUKASE, T. MASUMOTO
*The Research Institute for Iron, Steel and Other Metals, and *Graduate School, Tohoku University, Sendai 980, Japan*

A new type of refractory metal-metalloid amorphous alloys exhibiting superconductivity has been found in a binary Zr–Ge system by a modified melt-spinning technique. Specimens are in the form of continuous ribbons 1 to 2 mm wide and 0.02 to 0.03 mm thick. The germanium content in the amorphous alloys is limited to the range of 13 to 21 at %. These amorphous alloys are so ductile that no cracks are observed even after closely contacted bending test. The Vickers hardness and crystallization temperature increase from 435 to 530 DPN and from 628 to 707 K, respectively, with germanium content, and the tensile fracture strength is about 1460 MPa. Furthermore, the amorphous alloys exhibit a superconducting transition which occurs very sharply. The superconducting transition temperature (T_c) increases with decreasing germanium content and reaches a maximum value of 2.88 K for $Zr_{87}Ge_{13}$. The upper critical magnetic field for $Zr_{87}Ge_{13}$ alloy was of the order of 21.8 kOe at 2.0 K and the critical current density for $Zr_{85}Ge_{15}$ alloy was about 175 A cm^{-2} at 1.70 K in the absence of an applied field. The upper critical field gradient at T_c and the electrical resistivity at 4.2 K increase significantly from 24.6 to 31.5 kOe K^{-1} and from 235 to 310 $\mu\Omega$cm, respectively, with the amount of germanium. The Ginzburg–Landau (GL) parameter κ and the GL coherence length $\xi_{GL}(0)$ were estimated to be 72 to 111 and about 7.9 nm, respectively, from these experimental values by using the Ginzburg–Landau–Abrikosov–Gorkov (GLAG) theory and hence it is concluded that the Zr–Ge amorphous alloys are extremely "soft" type-II superconductor with high degree of dirtiness which possesses the T_c values higher than zirconium metal, in addition to high strength combined with good ductility.

1. Introduction

It is well known that germanium as well as boron, carbon, silicon and phosphorus is an amorphous phase-forming element. A large number of results on the formation and mechanical, physical and chemical properties of binary amorphous alloys containing a metalloid element of boron, carbon, silicon or phosphorus, etc., have been described (e.g. [1]) from the fundamental and technological points of view. However, the germanium-containing binary amorphous alloys are, within the authors' knowledge, only Pd–Ge [2] and La–Ge [3] systems and there are few informations about the effect of germanium on the amorphous phase formation and its resultant properties. It has been recently described [4–7] that an amorphous single phase forms in refractory metal (titanium, zirconium, hafnium or niobium)–silicon binary alloys quenched by a melt-spinning method and these amorphous alloys exhibit a superconductivity which has attracted an increased interest in recent years. The similarity of many properties between germanium and silicon suggests the possibility that an amorphous phase with superconductivity is obtained in refractory metal–germanium systems. The aim of this paper is to present the formation range and mechanical, thermal and superconducting properties of the Zr–Ge amorphous alloys and to compare their properties with those of binary Zr–Si amorphous alloys.

0022–2461/82/113299–09$03.58/0

2. Experimental methods

Binary zirconium–germanium alloys of different compositions ranging between 5 and 25 at% Ge were pre-alloyed under an argon atmosphere in an arc furnace on a water-cooled copper hearth with a non-consumable tungsten electrode from zirconium (99.6 wt%) containing 0.086 wt% oxygen and 0.051 wt% iron, etc., impurities and germanium (99.999 wt%). The weight of the mixture melted in one run was about 30 g. The ingots were repeatedly turned over and remelted to ensure homogeneity of composition. The compositions of alloys reported are the nominal ones since the losses during melting were negligible. Each ingot was cut into pieces which were then used to rapidly fabricate ribbons from the melt by melt spinning under an argon atmosphere. Details of the apparatus have been described by Inoue and co-workers [4, 7]. Samples thus formed had a typical cross-section of about 20 μm x 1 mm. The ribbons were subjected to ductility testing by simple bend method in both the as-quenched state and after 1-hour anneals in the temperature range between 473 and 773 K. Samples able to sustain a 180° bend were designated as being ductile. The amorphous nature of as-quenched and annealed samples was examined by conventional X-ray diffraction, differential scanning calorimetry (DSC) and transmission electron microscopy (TEM) techniques. TEM specimens were prepared by electrolytically thinning ribbons in a 1:19 volumetric ratio of sulphuric acid: methanol solution immersed in liquid nitrogen. Hardness and tensile fracture strength were measured by a Vickers microhardness tester with a 100 g load and an Instron-type tensile testing machine at a strain rate of 1.7×10^{-4} sec^{-1}. All measurements of the superconducting properties were done resistively using a four-point technique and the methods have been described in detail by Toyota *et al.* [8].

3. Results

3.1. Formation range of amorphous phase

The composition range in which the amorphous phase forms in the Zr–Ge binary system is shown in Fig. 1, wherein the equilibrium phase diagram is also represented for comparison. The amorphous phase forms in the rather wide range of 13 to 21 at% Ge. Furthermore, it can be seen in Fig. 1 that the alloys containing germanium ranging between 9 and 12 at%, exhibit a non-equilibrium crystalline phase with a b c c structure.

In general, the amorphous phase-forming range of metal–metalloid type alloys is located in the

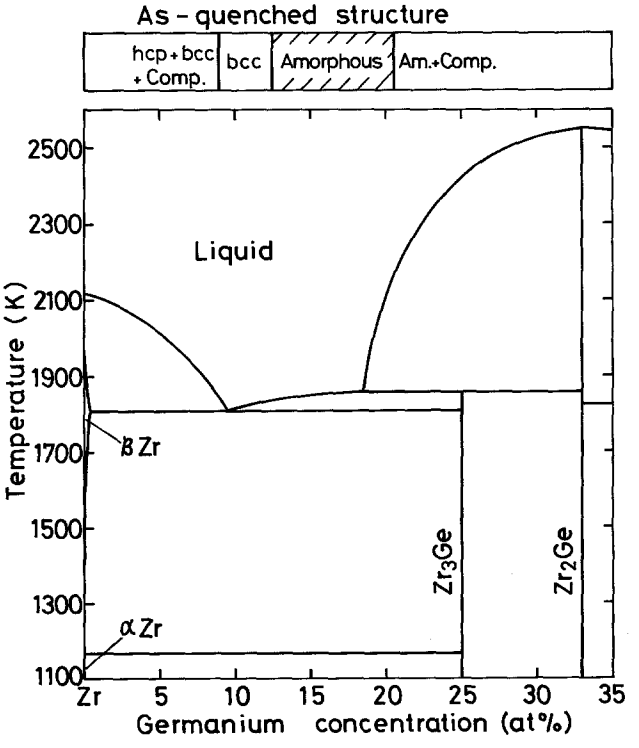

Figure 1 Composition range for the formation of an amorphous phase in Zr–Ge binary system. Binary phase diagram was adopted from Hansen [9].

range encompassing a eutectic composition [10]. The high amorphous phase-forming tendency appears to be due to the lowering of T_m and the increase of T_g through a comparatively large negative heat of formation around a deep eutectic [11]. However, the eutectic $Zr_{91.5}Ge_{9.5}$ alloy exhibits only the b c c phase as shown in Fig. 1 and the amorphous phase-formation range lies in the composition range between the eutectic point and the Zr_3Ge compound. This result suggests that a strong chemical bonding nature between metal and metalloid atoms plays an important role in forming an amorphous phase, in addition to the deep trough of melting temperature. The formation of an amorphous phase in binary alloys is commonly limited to the metalloid range of about 13 to 30 at% [12]. Furthermore, it has been pointed out from the structural point of view [13] that the dissolution of about 20 at% metalloid is necessary for the formation of stable amorphous phase around room temperature. Therefore, it may be said that the germanium content (9.5 at%) at the eutectic composition is too low to reach the level of the interaction between zirconium and germanium required for the formation of the amorphous phase.

3.2. Mechanical strengths and thermal stability

Zirconium–germanium amorphous ribbons containing less than about 17 at% Ge produced in the present investigation exhibited good bend ductility. When a $Zr_{85}Ge_{15}$ amorphous alloy is completely bent by pressing around the edge of a thin razor blade, the generation of numerous deformation markings is seen near the bent edge, but no cracks can be observed even after such a severe deformation. The good ductility for $Zr_{85}Ge_{15}$ alloy remained unchanged upon annealing for 3.6×10^3 sec at temperatures up to about 630 K.

Vickers hardness (H_v), tensile fracture strength (σ_f), crystallization temperature (T_{x1} and T_{x2}) and the activation energy for crystallization (ΔE) are presented in Table I. The H_v and σ_f values are the average over seven measurements and the T_{x1} or T_{x2} is defined as the temperature corresponding to the start of the first or second exothermic peak on the DSC curve measured at a heating rate of 20 K min^{-1}. Since the majority of the exothermic amount for crystallization is occupied by the second peak corresponding to the precipitation of Zr_3Ge compound [14] as shown in Fig. 2, ΔE was calculated by measuring the position of the second peak at different heating rates by the Kissinger method [15]. The H_v gradually increases with the amount of germanium and reaches about 530 DPN for $Zr_{82}Ge_{18}$ alloy probably because of the increase in the number of bonding between zirconium and germanium atoms which are considered to have rather strongly attractive interaction. The fracture strength is about 1460 MPa for $Zr_{85}Ge_{15}$ alloy. The T_x shows the same composition dependence as the H_v values and increases from 628 to 707 K. On the other hand, the ΔE value decreases slightly from 195 to 180 kJ mol^{-1} with the amount of germanium. The significant increase of T_x is due to the disappearance of the first broad peak corresponding to the precipitation of b c c β-Zr phase as shown in Fig. 2. Furthermore, the reason for the decrease of ΔE appears to be due to the tendency that the precipitation of the β-Zr phase is suppressed with the amount of germanium and the precipitation of Zr_3Ge compound becomes easy.

3.3. Superconducting properties

Electrical resistance of several Zr–Ge amorphous alloys at low temperatures was measured in the absence of applied field and the transition behaviour of normal to superconducting state is shown in Fig. 3. The transition occurs very sharply within a temperature width less than 0.1 K, indicating that these alloys possess very homogeneous structure on the scale of coherence length. The

TABLE I Vickers hardness (H_v), tensile fracture strength (σ_f), crystallization temperature (T_{x1} and T_{x2}), the activation energy for crystallization (ΔE) and the critical fracture temperature upon 1-h annealing (T_f) for Zr–Ge amorphous alloys

Alloys	H_v(DPN)	σ_f(MPa)	T_{x1}(K)	T_{x2}(K)	ΔE(kJ mol^{-1})	T_f($K \times 3.6 \times 10^3$ sec)
$Zr_{87}Ge_{13}$	435	–	628	762	195	–
$Zr_{85}Ge_{15}$	450	1460	635	743	187	630
$Zr_{83}Ge_{17}$	515	–	690	722	180	–
$Zr_{82}Ge_{18}$	530	–	–	707	–	–

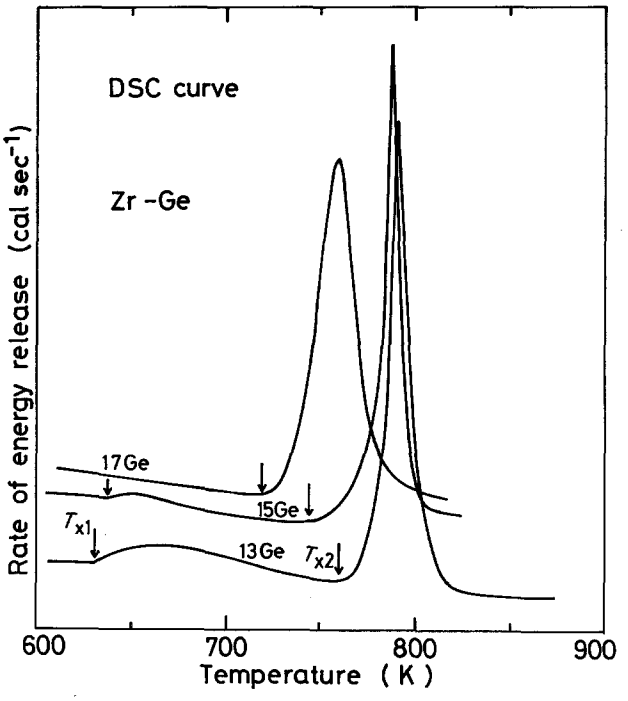

Figure 2 Differential scanning calorimetric curves of $Zr_{87}Ge_{13}$, $Zr_{85}Ge_{15}$ and $Zr_{83}Ge_{17}$ amorphous alloys.

electrical resistivity in normal state increases significantly with increasing germanium content and reaches an extremely high value of about 310 $\mu\Omega$cm for $Zr_{83}Ge_{17}$ alloy. One can also see the tendency that the lower the electrical resistivity the higher is the superconducting transition temperature (T_c) and the larger is the transition width (ΔT_c). The values of T_c and ΔT_c are plotted as a function of germanium content in Fig. 4, where the data of the non-equilibrium bcc solid solution are also shown for reference. The T_c values are those of the transition midpoint and the transition width ΔT_c is the difference between the 10% and 90% points. The T_c and ΔT_c values increase from 2.05 to 2.88 K and from 0.03 to 0.07 K, respectively, with decreasing germanium content. The T_c values are about 3.4 to 4.7 times as high as that (0.61 K) [16] of zirconium metal and the highest value is almost the same level as the highest value ($\simeq$ 3.0 K) [17] of amorphous zirconium metal obtained by vapour-deposition on to a cryogenic substrate,

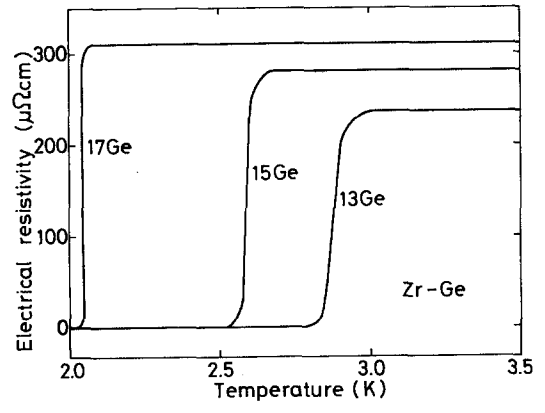

Figure 3 Change in electrical resistivity as a function of temperature for $Zr_{87}Ge_{13}$, $Zr_{85}Ge_{15}$ and $Zr_{83}Ge_{17}$ amorphous alloys.

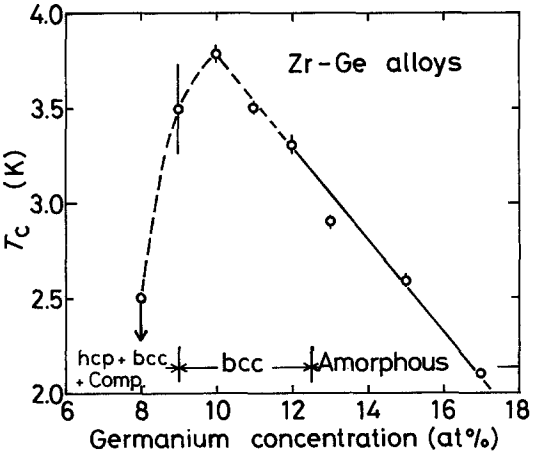

Figure 4 Changes in the superconducting transition temperature (T_c) and the transition width (ΔT_c) for Zr–Ge amorphous alloys with germanium content. Vertical bars represent the transition width and downward arrow indicates no superconductivity down to $T = 2.5$ K.

in spite of the dissolution of a rather large amount of germanium which is a nonsuperconducting element in atmospheric pressure. Thus, the zirconium amorphous alloys are interesting on the point that the superconductivity is superior for the amorphous state than for the equilibrium state, similar to the molybdenum-based amorphous alloys [18]. Furthermore, it may be important to note that the replacement of the amorphous phase by the b c c solid solution results in a further increase of T_c to 3.88 K, but the value significantly decreases by the appearance of the mixed structure consisting of b c c β-Zr(Ge), h c p α-Zr and unidentified Zr–Ge compound and the $Zr_{92}Ge_8$ alloy with the mixed structure remains in a normal state down to a temperature as low as 2.5 K. The details of the superconductivity of the b c c solid solution will be described elsewhere in the near future.

Resistive curves as a function of magnetic field at different temperatures for the $Zr_{85}Ge_{15}$ amorphous alloy are shown in Fig. 5, wherein the H_{c2} value was defined as the applied field at which the resistance of the sample begins to deviate from its normal value. Resistive states are seen in the wide range of fields, following the sharp dips as the field approaches H_{c2}. The H_{c2} values of the Zr–Ge amorphous alloys are plotted in Fig. 6 as a function of temperature. When the H_{c2} value is compared at the same temperature, the value increases with decreasing germanium content, following the general tendency that the higher the T_c, the higher is H_{c2} (e.g. [19]). For all the samples, there exists a linear relationship between H_{c2} and temperature in the temperature range just below T_c. The gradient at T_c, $(dH_{c2}/dT)_{T_c}$, is estimated to be -24.6 kOe K^{-1} for $Zr_{87}Ge_{13}$, -28.7 kOe K^{-1} for $Zr_{85}Ge_{15}$ and -31.5 kOe K^{-1} for $Zr_{83}Ge_{17}$, being much larger than that for crystalline superconducting alloys such as Ti–Nb and Zr–Nb. One can also see the tendency that the gradient values at T_c increase with in-

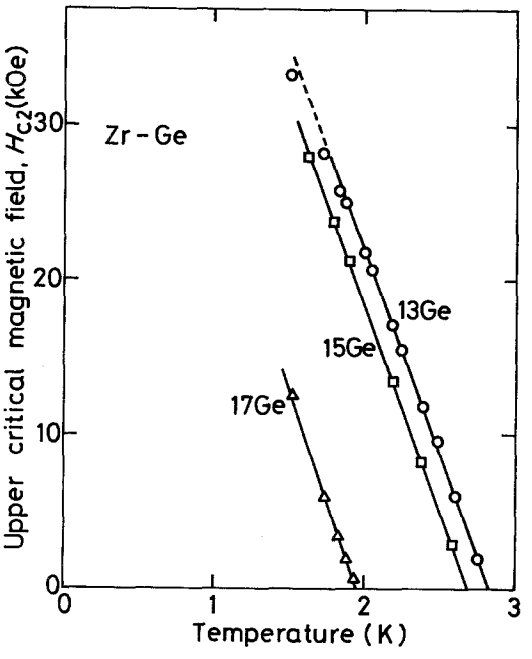

Figure 6 Change in the upper critical magnetic field H_{c2} as a function of temperature for $Zr_{87}Ge_{13}$, $Zr_{85}Ge_{15}$ and $Zr_{83}Ge_{17}$ amorphous alloys.

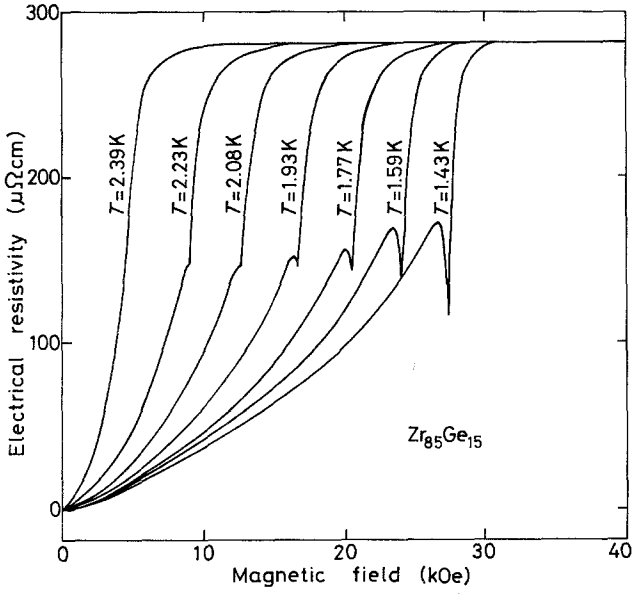

Figure 5 Change in electrical resistance at various temperatures as a function of magnetic field for $Zr_{85}Ge_{15}$ amorphous alloy.

creasing germanium content and electrical resistivity. The J_c of the $Zr_{85}Ge_{15}$ alloy was measured at several temperatures as a function of magnetic field and the result is plotted in Fig. 7. The critical current is defined as the threshold current at which no zero voltage ($\simeq 1\,\mu V$) is first detected. The J_c value at $H = 0$ is about 175 A cm^{-2} at 1.70 K and about 140 A cm^{-2} at 2.00 K. The value begins to decrease with the applied field and falls to about 40 A cm^{-2} at 1.70 K and about 35 A cm^{-2} at 2.00 K in the applied field of $H \simeq 0.75\,H_{c2}$. Thus, the $Zr_{85}Ge_{15}$ amorphous alloy exhibit extremely small values of $J_c(H)$, which are about one-tenth to one-hundredth as large as the molybdenum-based amorphous superconductors [18], and hence this alloy is considered to be very "soft" type of superconductors. Such small values seem to originate from the results that the present sample possesses a strict homogeneity of the amorphous structure on the scale of coherence length (which is estimated to be about 7.9 nm in the next section) and flux pinning interactions are very weak.

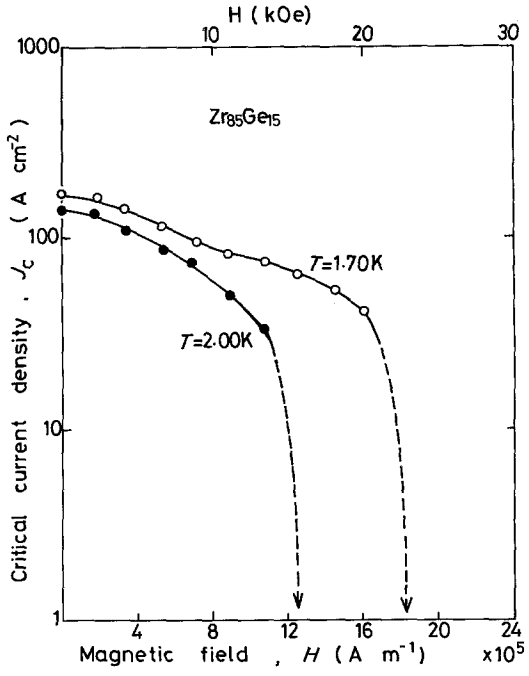

Figure 7 Change in the critical current density J_c as a function of magnetic field for $Zr_{85}Ge_{15}$ amorphous alloy.

4. Discussion

4.1. Comparison of the amorphous phase-formation range between Zr–Ge and Zr–Si systems

We shall briefly compare the formation range of binary Zr–Ge and Zr–Si amorphous alloys which contain an analogous type of metalloid. In a previous paper, we described that the amorphous phase in binary Zr–Si alloys formed in the silicon range of 12 to 24 at%. Therefore, the main difference of the formation range is the following two points; (a) the formation range of Zr–Ge amorphous alloys is narrower than that of Zr–Si amorphous alloys, and (b) the maximum metalloid content is considerably lower for Zr–Ge alloys than for Zr–Si alloys. In Section 3.1., it was described how the lowering of T_m and the strong interaction between metal and metalloid play an important role on the amorphous-phase formation of metal–metalloid alloys. The eutectic temperature is 1883 K for Zr–Si alloys and 1808 K for Zr–Ge alloys, being lower for the latter alloys. Nevertheless, the formation range of the amorphous phase is narrower for the Zr–Ge alloys than for the Zr–Si alloys, suggesting that the amorphous-phase formation is not controlled only by the lowering of T_m. According to the equilibrium phase diagrams [9] of Zr–Si and Zr–Ge alloys, the formation of metal–metalloid compound is seen at 20 at% (Zr_4Si) for the Zr–Si system and at 25 at% Ge (Zr_3Ge) for the Zr–Ge system. This indicates that the formation tendency of the compound is weaker for Zr–Ge alloys than for Zr–Si alloys, resulting in a weaker interaction between metal and metalloid atoms. Therefore, the narrower formation range of Zr–Ge amorphous alloys appears to be due to the weaker interaction between zirconium and germanium. The maximum metalloid content of Zr–Ge amorphous alloys is also considerably lower than that of Zr–Si amorphous alloys. This may be reasonably explained by the inference that germanium has an atomic size larger than silicon and hence the solid solubility limit in amorphous phase was suppressed to a lower value for the Zr–Ge alloys than for the Zr–Si alloys.

4.2. Relation between ρ_n and T_c, ΔT_c or $(dH_{c2}/dT)_{T_c}$

The experimental values of T_c, ΔT_c and $(dH_{c2}/dT)_{T_c}$ for amorphous Zr–Ge alloys are plotted as a function of electrical resistivity ρ_n at 4.2 K in Fig. 8. There is a clear tendency that the T_c and ΔT_c values are reduced and the value of $(dH_{c2}/dT)_{T_c}$ increases with increasing electrical

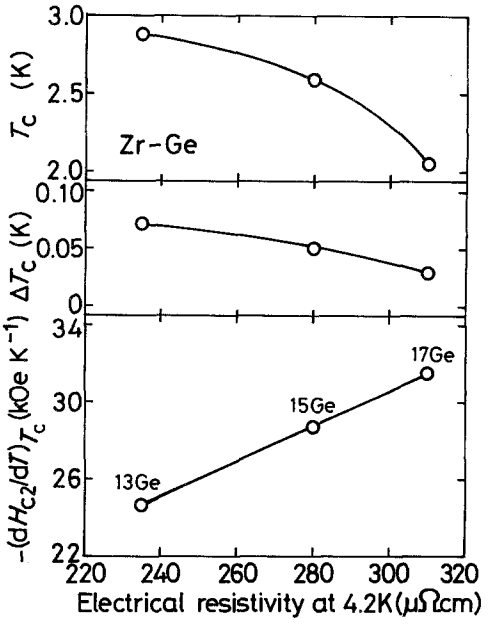

Figure 8 Relation between ρ_n and T_c, ΔT_c or $(dH_{c2}/dT)_{T_c}$.

resistivity. In general, amorphous superconductors have the features that the superconducting transition sharply occurs from an extremely high resistive state and the H_{c2} value rapidly increases with lowering temperature [20]. Hence, it is said that the features of the superconductivity for the Zr–Ge alloys become more remarkable with the increase in electrical resistivity and/or germanium content. Although the reason for the increase in electrical resistivity with germanium content is not clear, it may be due to the combined effect of the following two factors: (a) the increase of germanium element exhibiting a semiconducting nature, and (b) the increase of structural disorder in the amorphous phase with the amount of germanium. Anyhow, it is concluded that the increase in the metalloid content in an amorphous phase endows superconductivity having a more typical amorphous-like nature through the increase in electrical resistivity.

4.3. Dominating parameters for T_c

According to McMillan [21], T_c depends on the Debye temperature θ_D and the electron–phonon coupling constant λ or the electronic bare density of states $N(E_f)$ and the larger the θ_D, λ and $N(E_f)$ the higher is the T_c. T_c is especially strongly influenced by λ compared with θ_D, and hence it is expected that the T_c is closely related with λ and/or $N(E_f)$. Usually, the value of $N(E_f)$ is determined from measurements of low-temperature specific heat, magnetic susceptibility and photoemission, etc. In this study, we estimated the electronic dressed density of states $N^*(E_f) = N(E_f)(1+\lambda)$ and the electronic specific heat coefficient, γ, from the measured values of the upper critical field gradient at T_c, $(dH_{c2}/dT)_{T_c}$, and electrical resistivity at 4.2 K, ρ_n, by using the following relations based on the Ginzburg–Landau–Abrikosov–Gorkov (GLAG) theory (e.g. [22]).

$$\gamma = -\frac{\pi^3 k_B}{12 e \rho_n}\left(\frac{dH_{c2}}{dT}\right)_{T_c} \quad (1)$$

$$N^*(E_f) = \frac{3\gamma}{2\pi^2 k_B^2} \quad (2)$$

Values of γ and $N^*(E_f)$ thus obtained are summarized in Table II, together with the values of T_c, dH_{c2}/dT at T_c and ρ_n. The γ and $N^*(E_f)$ values for Zr–Ge amorphous alloys increase from 2270 to 2890 erg cm^{-3} K^{-2} and from 1.81×10^{34} to 2.30×10^{34} states cm^{-3} erg^{-1} spin^{-1}, respectively, with decreasing germanium content. The relation between T_c and γ is shown in Fig. 9. It can be seen that the values of γ are reflected in T_c: that is, the larger the values of γ and/or $N^*(E_f)$, the higher is T_c. However, the γ values of the Zr–Ge amorphous alloys are

TABLE II Superconducting and the related properties for Zr–Ge amorphous alloys. The data for $Zr_{85}Si_{15}$ amorphous alloy are also shown for [24]

Alloys	T_c(K)	ΔT_c(K)	ρ_n, 4.2 K (μΩcm)	$-(dH_{c2}/dT)_{T_c}$ (kOe K^{-1})	γ	$N^*(E_f)$ $\times 10^{34}$	κ	$\xi_{GL}(0)$ (nm)	λ_0 (nm)	D (cm^2 sec^{-1})
$Zr_{87}Ge_{13}$	2.88	0.07	235	24.6	2340	1.86	85	8.0	950	0.446
$Zr_{85}Ge_{15}$	2.59	0.05	280	28.7	2290	1.82	101	7.8	1090	0.382
$Zr_{83}Ge_{17}$	2.05	0.03	310	31.5	2270	1.81	111	8.3	1200	0.348
$Zr_{85}Si_{15}$	2.71	0.05	270	28.9	2390	1.90	100	6.6	1050	0.390

γ: (erg cm^{-3} K^{-2}), $N^*(E_f)$: (states cm^{-3} erg^{-1} spin^{-1})

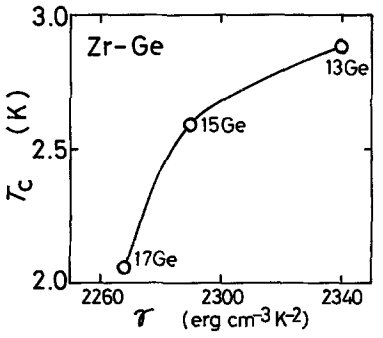

Figure 9 Relation between T_c and γ for Zr–Ge amorphous alloys.

slightly lower than that (2486 erg cm^{-3} K^{-2}) [16] of zirconium metal. This degradation is due to the extremely high electrical resistivities of the amorphous alloys as evident from Equation 1. Nevertheless, the zirconium-based amorphous alloys exhibit T_c values higher than that of zirconium metal. More recently, it has been demonstrated for Zr–Nb–Si amorphous alloys [23] that the higher T_c values for the amorphous state are due to the high λ values for zirconium-based amorphous alloys exhibiting a strong-coupling type superconductor. A similar mechanism appears to be reflected in higher T_c values for the Zr–Ge amorphous state.

4.4. Parameters characterizing the amorphous superconductor

The GL coherence length, ξ_{GL}, the penetration depth, λ_0, the extrinsic GL parameter, κ, and the electronic diffusivity, D, were estimated by using the following relations derived from an extended GLAG theory for "dirty" superconductors and their values are also shown in Table II.

$$\xi_{GL}(0) = 1.0 \times 10^{-6}(\rho_n \gamma T_c)^{-1/2} \quad (3)$$

$$\lambda_0 = 1.05 \times 10^{-2}(\rho_n/T_c)^{1/2} \quad (4)$$

$$\kappa = 7.49 \times 10^3 \gamma^{1/2} \rho_n \quad (5)$$

$$D = \frac{4k_B c}{\pi e}\left(\frac{dH_{c2}}{dT}\right)^{-1}_{T_c} \quad (6)$$

As shown in the table, the κ and λ_0 increase from 72 to 111 and 775 to 1290 nm, respectively, with the amount of germanium, while the D value decreases inversely from 0.47 to 0.35 cm^2 sec^{-1}. No clear change of the $\xi_{GL}(0)$ is observed and the value is about 7.9 nm. Such high values of κ, $\xi_{GL}(0)$ and λ_0 and the low value of D appear to originate from a small value of the electron mean free path, l, due to the disordered structure near atomic scale, as evidenced by the high electrical resistivity ranging from 235 to 310 $\mu\Omega$cm. Therefore, it is concluded that the present Zr–Ge amorphous superconductors are typical type-II material characterized as extremely high degree of dirtiness. In addition, the degree of dirtiness significantly increases with the amount of germanium, and the κ value for the $Zr_{83}Ge_{17}$ amorphous alloy is considerably larger than that (50 to 100) of the other amorphous superconductors, suggesting that atomic configurations in the present amorphous alloys are in a more random state on a scale much smaller than $\xi_{GL}(0)$.

Finally, the superconductivity and related properties of amorphous $Zr_{85}Ge_{15}$ and $Zr_{85}Si_{15}$ alloys [8, 24] are compared as summarized in Table II. The T_c value of the $Zr_{85}Ge_{15}$ alloy is lower only by 0.12 K than that of the $Zr_{85}Si_{15}$ alloy. Although the difference is very small, it appears to be closely related to the result that the γ and/or $N^*(E_f)$ values are slightly lower for the former alloy. However, the other superconducting parameters are almost the same between both alloy systems. Hence, it may be concluded that the superconducting parameters of the zirconium-based binary amorphous alloys hardly change by complete replacement of germanium with silicon.

5. Conclusion

A new type of amorphous alloys exhibiting superconductivity and high strength combined with a highly ductile nature was found in the Zr–Ge binary system. Samples were fabricated in the form of a continuous ribbon of about 1 mm wide and about 20 μm thick using a melt-spinning apparatus designed for high melting point alloys. The amorphous single phase was obtained in the composition range between about 13 and 21 at% Ge. The Vickers hardness and tensile fracture strength were in the range of 435 to 530 DPN and about 1460 MPa, respectively. Crystallization temperature and the activation energy for crystallization varied from 628 to 707 K and from 195 to 180 kJ mol^{-1}, respectively, with the amount of germanium. Furthermore, these amorphous alloys were able to sustain a 180° bend and the ductility remained unchanged for 3.6×10^3 sec^{-1} at temperatures below about 630 K for $Zr_{85}Ge_{15}$ alloy. In addition, the Zr–Ge

alloys showed a sharp superconducting transition from extremely high electrical resistivities. The transition temperature T_c increased from 2.05 to 2.88 K with decreasing germanium content, being much higher than that of zirconium metal. The same tendency was recognized for the H_{c2} and J_c. The values of H_{c2} and J_c for the $Zr_{85}Ge_{15}$ alloy were of the order of 18.3 kOe at 2.0 K and 175 A cm^{-2} at 1.70 K and in the absence of an applied field. The dH_{c2}/dT at T_c and ρ_n at 4.2 K varied from 24.6 to 31.5 kOe K^{-1} and 235 to 310 $\mu\Omega$cm, respectively, with increasing germanium content. The $\xi_{GL}(0)$ and κ were estimated to be about 7.9 nm and 72 to 111, respectively, from the data of $(dH_{c2}/dT)_{T_c}$ and ρ_n, using the extended GLAG theory and it was therefore concluded that the present amorphous alloys are typical type-II superconductor with an extremely high degree of dirtiness.

References

1. H. S. CHEN, *Rep. Prog. Phys.* **43** (1980) 353.
2. N. HAYASHI, T. FUKUNAGA, M. UENO and K. SUZUKI, *Res. Rep. Lab. Nucl. Sci. Tohoku Univ.* **13** (1980) 249.
3. K. AGYEMAN, R. MULLER and C. C. TSUEI, *Phys. Rev. B* **19** (1979) 193.
4. A. INOUE, H. M. KIMURA, S. SAKAI and T. MASUMOTO, Proceedings of the Fourth International Conference on Titanium, edited by H. Kimura and O. Izumi (ASM, Metals Park, Ohio, 1980) p. 1137.
5. A. INOUE, Y. TAKAHASHI and T. MASUMOTO, *Sci. Rep. Res. Inst. Tohoku Univ.* **A-29** (1981), 296.
6. A. INOUE, Y. TAKAHASHI, C. SURYANARAYANA and T. MASUMOTO, *J.Mater. Sci.* **17** (1982) 1753.
7. T. MASUMOTO, A. INOUE, S. SAKAI, H. M. KIMURA and A. HOSHI, *Trans. Japan Inst. Metals* **21** (1980) 115.
8. N. TOYOTA, T. FUKASE, A. INOUE, Y. TAKAHASHI and T. MASUMOTO, *Physica* **107B** (1981) 465.
9. M. HANSEN, "Constitution of Binary Alloys" (McGraw-Hill, New York, 1958) p. 780.
10. H. S. CHEN and K. A. JACKSON, "Metallic Glasses" (ASM, Metals Park, Ohio, 1978) p. 74.
11. D. TURNBULL, *J. Phys. Colloque-4* **35** (1974) 1.
12. H. A. DAVIES, *Phys. Chem. Glasses* **17** (1976).
13. D. E. POLK, *Scripta Metall.* **4** (1970) 117.
14. A. INOUE and T. MASUMOTO, unpublished research (1981).
15. H. E. KISSINGER, *Anal. Chem.* **29** (1957) 1702.
16. R. W. ROBERTS, "Properties of Selected Superconductive Materials", 1978 Supplement, NBS Tech. Note 983, p. 12.
17. M. M. COLLVER and R. H. HAMMOND, *Phys. Rev. Lett.* **30** (1973) 92.
18. E. R. DOMB and W. L. JOHNSON, *J. Low Temp. Phys.* **33** (1978) 29.
19. K. MAKI and T. TSUZUKI, *Phys. Rev.* **139** (1965) 868.
20. W. L. JOHNSON, "Rapidly Quenched Metals III", edited by B. Cantor, (The Metals Society, London, 1978) p. 2.
21. W. L. MCMILLAN, *Phys. Rev.* **167** (1968) 331.
22. T. R. ORLANDO, E. J. MCNIFF, Jr, S. FONER and M. R. BEASLEY, *Phys. Rev. B* **19** (1979) 4545.
23. A. INOUE, Y. TAKAHASHI, N. TOYOTA, T. FUKASE and T. MASUMOTO, *J. Mater. Sci.* in press.
24. A. INOUE, Y. TAKAHASHI, N. TOYOTA, T. FUKASE and T. MASUMOTO, in "Proceedings of the Fourth International Conference on Rapidly Quenched Metals", edited by T. Masumoto and K. Suzuki (The Japan Institute of Metals, Sendai, 1982) p. 1221.

Received 30 March
and accepted 23 April 1982